

Zero-sound mode in a neutral Fermi liquid: dynamic fermionic correlations applied to two-dimensional ^3He

M. Nava¹, D.E. Galli¹, S. Moroni², and E. Vitali¹

¹ *Dipartimento di Fisica, Università degli Studi di Milano, via Celoria 16, 20133 Milano, Italy*

² *IOM-CNR DEMOCRITOS National Simulation Center, via Beirut 2-4, 34014 Trieste, Italy*

(Dated: April 20, 2019)

Recent neutron scattering experiments on ^3He films have observed a zero-sound mode, its dispersion relation and its merging with –and possibly emerging from– the particle-hole continuum. We develop a practical quantum Monte Carlo scheme to calculate imaginary time correlation functions for moderate-size fermionic systems. Combined with an efficient method for analytic continuation, this scheme affords an extremely convincing description of the experimental findings.

PACS numbers: 67.30.ej, 67.30.em, 02.70.Ss

Introduction: The two isotopes of Helium, ^3He and ^4He , give the opportunity to explore the quantum behavior of many-body systems on a fundamental basis; at low temperature and pressures, they are the only neutral quantum liquids existing in Nature and an impressive complexity of physical phenomena is generated by merely pair interactions between particles and the effects of quantum statistics. In the investigation of the fascinating behavior of strongly correlated quantum systems a key role is naturally played by the low energy dynamics (see, for example, Ref. 1). In addition, due to the very simple Hamiltonian, ^3He and ^4He many-body systems represent also extremely important reference models and test cases for general theoretical approaches².

Recently inelastic neutron scattering experiments have been performed on a monolayer of liquid ^3He adsorbed on suitably preplated graphite: a collective *zero-sound* mode (ZSM) has been detected as a well defined excitation crossing and possibly reemerging from the particle-hole continuum typical of a Fermi fluid^{3,4}. The aim of this work is to undertake an *ab-initio* study of the ZSM in a strictly two-dimensional (2D) ^3He sample relying on Quantum Monte Carlo (QMC) methods. It has been shown that this ideal, strictly 2D model offers a realistic representation of the adsorbed liquid layer, as far as the liquid phase properties are concerned^{5–7}.

The key quantity to be computed to compare with the ZSM observed in neutron scattering experiments on ^3He systems is the coherent dynamic structure factor⁸, which, apart from kinematical factors, is related to the differential cross section:

$$S(q, \omega) = \frac{1}{2\pi N} \int_{-\infty}^{+\infty} dt e^{i\omega t} \langle e^{i\frac{t}{\hbar}\hat{H}} \hat{\rho}_{\vec{q}} e^{-i\frac{t}{\hbar}\hat{H}} \hat{\rho}_{-\vec{q}} \rangle . \quad (1)$$

The brackets indicate a ground state or thermal average, \hat{H} is the Hamiltonian operator, and $\hat{\rho}_{\vec{q}} = \sum_{i=1}^N e^{-i\vec{q}\cdot\vec{r}_i}$ is the local density in Fourier space. The ZSM of the system manifests itself in the shape of $S(q, \omega)$, appearing either as sharp peaks if it is long-lived or as broad structures if strong damping is present¹.

QMC methods give access to the coherent dynamic structure factor, $S(q, \omega)$, because they allow to evaluate the intermediate scattering function $F(q, \tau) =$

$\langle e^{\tau\hat{H}} \hat{\rho}_{\vec{q}} e^{-\tau\hat{H}} \hat{\rho}_{-\vec{q}} \rangle$ by simulating the imaginary time dynamics driven by the Hamiltonian^{9,10}. For a collection of ^3He atoms, a very accurate microscopic description is afforded by the simple Hamiltonian

$$\hat{H} = -\frac{\hbar^2}{2m_3} \sum_{i=1}^N \nabla_i^2 + \sum_{i<j=1}^N v(|\vec{r}_i - \vec{r}_j|) . \quad (2)$$

where m_3 is the mass of ^3He atoms and $v(r)$ is an effective pair potential among ^3He atoms¹¹.

The correlation function $F(q, \tau)$ is the Laplace transform of $S(q, \omega)$. Despite the well known difficulties related to the inversion of the Laplace transform in ill-posed conditions, the evaluation of $S(q, \omega)$ starting from the QMC estimation of $F(q, \tau)$ (3) has been proved to be fruitful for several bosonic systems^{10,12–16}.

For a Fermi liquid, the difficulty is further enhanced by the famous *sign problem*¹⁷, thereby the computational effort grows exponentially with the imaginary time and with the number of particles. While accurate approximations exist to circumvent this problem in the calculation of static ground-state properties¹⁸, we are aware of no applications of approximate schemes such as the restricted path¹⁹ or constrained path²⁰ methods to the calculation of imaginary-time correlation functions.

Focusing on $T = 0$ K, QMC calculations of ground state average replaces the unknown exact ground state ψ_0 by the imaginary time projection of a trial function ψ_T ^{10,21,22}, $\psi_0 \equiv e^{-\lambda\hat{H}} \psi_T$. The intermediate scattering function then reads:

$$F(q, \tau) = \frac{\langle \psi_T | e^{-\lambda\hat{H}} \hat{\rho}_{\vec{q}} e^{-\tau\hat{H}} \hat{\rho}_{-\vec{q}} e^{-\lambda\hat{H}} | \psi_T \rangle}{\langle \psi_T | e^{-(2\lambda+\tau)\hat{H}} | \psi_T \rangle} . \quad (3)$$

Unfortunately, the projection time λ required to filter out the exact ground state from the trial function is usually larger than the range of τ needed to extract spectral information, so that the total imaginary time $2\lambda + \tau$ in Eq. (3) is too large for practical purposes. In this paper we propose two related approximations which avoid the extra time 2λ , whereby the calculation becomes feasible for a few tens ^3He atoms. The agreement with the measured dynamic structure factor is more than satisfactory.

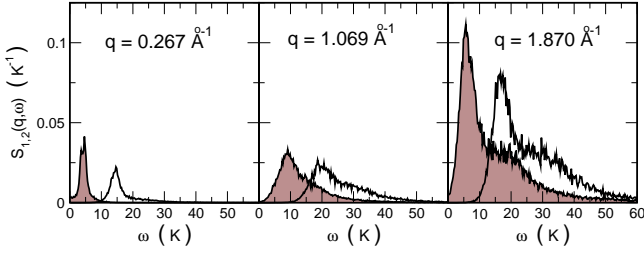


Figure 1: (Color online) Comparison between the spectral functions $S_1(q, \omega)$ (filled curve down to the baseline) obtained with the GIFT algorithm from $F_1(q, \tau)$ and $S_2(q, \omega)$ (unfilled curve) obtained from $F_2(q, \tau)$ with GIFT for some wave-vectors q at density $\rho = 0.047 \text{ \AA}^{-2}$. The two spectral functions have a compatible shape, with a shift in energy compatible with $E_0^F - E_0^B$.

The dynamic fermionic correlation method: We adopt the standard Jastrow-Slater form for the trial function, $\psi_T^F = \mathcal{J}D$. The starting point of the present work is the following approximation:

$$\psi_0^F = e^{-\lambda \hat{H}} \psi_T^F \simeq \mathcal{D} e^{-\lambda \hat{H}} \mathcal{J} = \mathcal{D} \psi_0^B \quad (4)$$

where ψ_0^F and ψ_0^B are respectively the fermionic and bosonic ground states of the Hamiltonian, (2). Throughout this paper, a superscript $F(B)$ indicates Fermi(Bose) statistics and a subscript 0 denotes the exact ground state. The convenience of the approximation (4) is that the extra projection time λ does not compound the sign problem because it is applied only to the symmetric factor of ψ_T^F . In the resulting approximate correlation function

$$F_1(q, \tau) = \frac{\langle \psi_0^B | \mathcal{D}^* \hat{\rho}_{\vec{q}} e^{-\tau \hat{H}} \hat{\rho}_{-\vec{q}} \mathcal{D} | \psi_0^B \rangle}{\langle \psi_0^B | \mathcal{D}^* e^{-\tau \hat{H}} \mathcal{D} | \psi_0^B \rangle} \quad (5)$$

the projection time between the determinants, which determines the severity of the sign problem, is limited to τ . $F_1(q, \tau)$ is an approximation of $F(q, \tau)$, and its inverse Laplace transform, $S_1(q, \omega)$, is an approximation of the coherent dynamic structure factor (1). The bias would vanish if $\mathcal{D} \psi_0^B$ were the exact Fermi ground state. The QMC calculation of F_1 requires the ratio of two correlation functions, $F_1(q, \tau) = F_2(q, \tau) / F_{\text{FC}}(\tau)$, where

$$F_{\text{FC}}(\tau) = \frac{\langle \psi_0^B | \mathcal{D}^* e^{-\tau \hat{H}} \mathcal{D} | \psi_0^B \rangle}{\langle \psi_0^B | e^{-\tau \hat{H}} | \psi_0^B \rangle} \quad (6)$$

and

$$F_2(q, \tau) = \frac{\langle \psi_0^B | \mathcal{D}^* \hat{\rho}_{\vec{q}} e^{-\tau \hat{H}} \hat{\rho}_{-\vec{q}} \mathcal{D} | \psi_0^B \rangle}{\langle \psi_0^B | e^{-\tau \hat{H}} | \psi_0^B \rangle} \quad (7)$$

Both $F_{\text{FC}}(\tau)$ and $F_2(q, \tau)$ are bosonic correlation functions and thus they can be evaluated with great accuracy by means of exact bosonic QMC methods. $F_{\text{FC}}(\tau)$ is precisely the correlation function that was recently

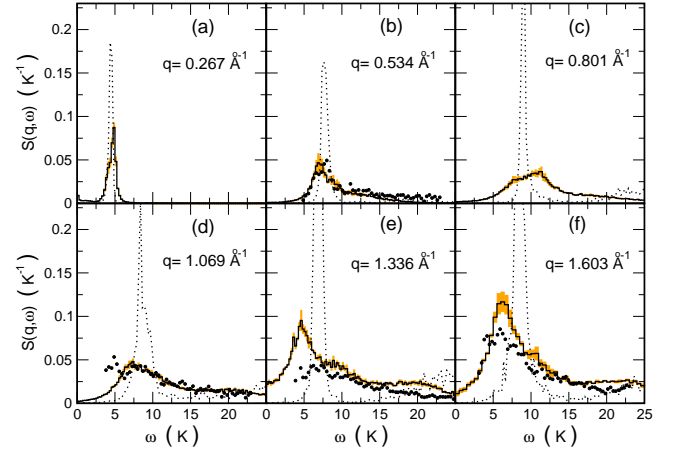


Figure 2: (Color online) From left to right the coherent dynamic structure factor, obtained as an average of several independently extracted $S_1(q, \omega)$, for increasing wave vectors at $\rho = 0.047 \text{ \AA}^{-2}$. The yellow shadows represents statistical uncertainties and filled circles are the available experimental data from Ref. 3 and Ref. 4. The wave-vector shown in picture are those accessible from our simulation, the experimental wave vectors are $q = 0.55 \text{ \AA}^{-1}$ (b), $q = 1.15 \text{ \AA}^{-1}$ (d), $q = 1.25 \text{ \AA}^{-1}$ (e) and $q = 1.65 \text{ \AA}^{-1}$ (f). The dotted line shows the dynamic structure factor of a fictitious system of bosons of mass m_3 .

used in the fermionic correlations (FC) method⁷ to study the magnetic properties of ^3He films. On the other hand, F_2 arises as an extension of the FC method to the calculation of the intermediate scattering function, hence the name “dynamic fermionic correlation” (DFC) for the present methodology. Indeed, the function F_2 possesses very interesting features on its own: on one hand, it contains the *exact* fermionic spectrum, as can be seen from its spectral resolution: $F_2(q, \tau) = \sum_{n=0}^{+\infty} e^{-\tau(E_n^F - E_0^B)} b_n$, where E_n^F are the fermionic energy eigenvalues, E_0^B is the bosonic ground state energy and $b_n = |\langle \hat{\rho}_{-\vec{q}} \mathcal{D} \psi_0^B | \psi_n^F \rangle|^2 / \langle \psi_0^B | \psi_0^B \rangle$. If, moreover, the approximation (4) is accurate enough, the coefficients b_n become, apart from an unessential normalization, the spectral weights of the exact intermediate scattering function, $F(q, \tau)$. Therefore, computing the inverse Laplace transform of F_1 and F_2 we can obtain two different estimations for the coherent dynamic structure factor, $S_1(q, \omega)$ and $S_2(q, \omega + E_0^F - E_0^B)$ respectively, where the shift in ω comes from the definition of F_2 in terms of the Bose ground state. A robust test for the validity of the approximation (4) is at hand if it turns out that $S_1(q, \omega) \simeq S_2(q, \omega + E_0^F - E_0^B)$: as already noticed, F_2 decays with the exact fermionic excitation energies (once shifted); moreover, if $\mathcal{D} \psi_0^B$ has a small overlap on the fermionic excited states, it follows that $e^{-\tau \hat{H}} \mathcal{D} \psi_0^B$ will quickly converge in τ to $e^{-\tau E_0^F} \psi_0^F$. Therefore $F_1(q, \tau) \simeq e^{\tau E_0^F} F_2(q, \tau)$, apart from an unessential normalization. We have indeed verified that, in the present case, $S_1(q, \omega)$ and $S_2(q, \omega + E_0^F - E_0^B)$ possess a

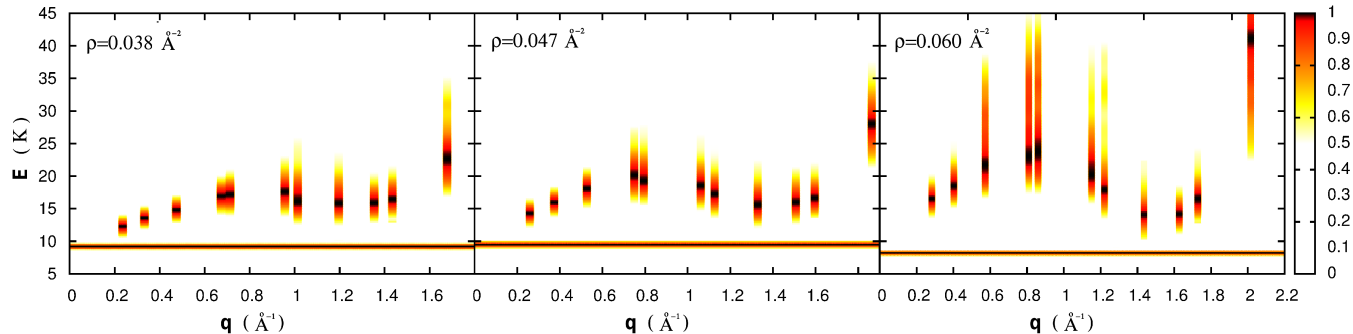


Figure 3: (Color online) Color map of normalized $S_2(q, \omega)$ for many wave vector q . For better visibility, each $S_2(q, \omega)$ for different q has been normalized in order to have their maximum value equal to 1. The horizontal continuous line represents the peak in the normalized spectral function extracted via GIFT from $F_{\text{FC}}(\tau)$, which corresponds to the energy gap between the Fermionic and the Bosonic ground state; it has been spread over all the q range in order to show the baseline energy value of the ZSM.

very similar shape (see Fig.1).

Results: We studied a system of $N = 26$ structureless 1/2-spin fermions of mass m_3 , interacting via the Aziz potential¹¹, enclosed in a square box with periodic boundary conditions. We found in Ref. 7 that this system size offers a good compromise between finite-size effects and computational cost. Indeed the inverse Laplace transform becomes increasingly difficult as the range of fermionic energy eigenvalues relevant for the spectral reconstruction departs from the reference energy of the underlying simulation, which is the bosonic ground state E_0^B : this is precisely what happens as the system size increases because the gap $E_0^F - E_0^B$ is an extensive quantity. The trial function $\psi_T^F = \mathcal{J}D$ is the same as in Ref. 7, namely a two-body Jastrow factor \mathcal{J} and a Slater determinant D of plane waves with simple backflow correlations. We have focused on a density around 0.047 \AA^{-2} , close to the experimental conditions³. Moreover, we have explored the behavior of the sample at the densities 0.038 and 0.060 \AA^{-2} in order to investigate the density-dependence of the excitations of the system. In particular, the highest density was chosen very close to the freezing point⁷. The QMC evaluation of F_2 requires a simple generalization of the methodology we have followed in Ref. 7 to compute F_{FC} : a fictitious system of *bosons* of mass m_3 is simulated by an *exact* projector Monte Carlo technique, the Shadow Path Integral Ground State²³. The imaginary-time propagation was a Pair Product⁹ with imaginary-time-step of $1/160 \text{ K}^{-1}$. It is well known that, in order to extract information from imaginary time correlation function, an inversion of the Laplace transform in ill-posed conditions is necessary. This can be carried out by means of the Genetic Inversion via Falsification of Theories (GIFT)¹³, which has been used to retrieve nontrivial spectral features in the study of low energy excitations of Bose superfluids^{13,14,16} and supersolids¹⁵.

In Fig. 2 we show the comparison between our estima-

tion of the dynamic structure factor of the ^3He film and the experimental data^{3,4}. The dynamic structure factor has been obtained as an average over several GIFT reconstructions of $S_1(q, \omega)$ from independent estimates of $F_1(q, \tau)$; this has made possible an estimation of the statistical uncertainties which we have shown in Fig. 2 with a yellow shadow. We note that the available experimental wave-vectors do not exactly match the reciprocal space grid defined by the simulation box. For $q = 0.534$ and $q = 1.603 \text{ \AA}^{-1}$, where the mismatch is minimal, a direct comparison is possible and the agreement is impressive. Inspection of the wave-vector dependence of the spectra shows that the discrepancies seen at $q = 1.069$ and $q = 1.336$ are mostly due to the differences of q values between theory and experiment. A major feature of the measured $S(q, \omega)$ is the appearance of a low-energy peak for both small and large wavevector, interpreted in Refs.3,4 as a well defined collective mode, broadened in the intermediate q range because of mixing with the particle-hole continuum. In further agreement with the measurements, we find a similar behavior. Indeed the simulation can provide information even at small wave vectors, not accessible to the experimental probe: at $q = 0.267$ the collective excitation (ZSM) is most pronounced, and the spectral weight of the particle-hole is negligible. It is remarkable that both the position and the shape of the calculated spectra have a physical meaning and are not artifacts of the reconstruction procedure. Further support to this conclusion is offered from a comparison with the dynamic structure factor of the fictitious ^3He -mass bosonic system. The bosonic spectrum has a completely different behavior, featuring an extremely sharp peak with the usual phonon-maxon-rotor dispersion, showing that the broadening of the fermionic spectrum is actually related to Fermi statistics.

In Fig.3 we report, in a color plot, the estimated $S_2(q, \omega)$. In agreement with the behavior of S_1 shown in Fig.2, at low q we find well defined excitation energies; as the wave vector increases, again we observe

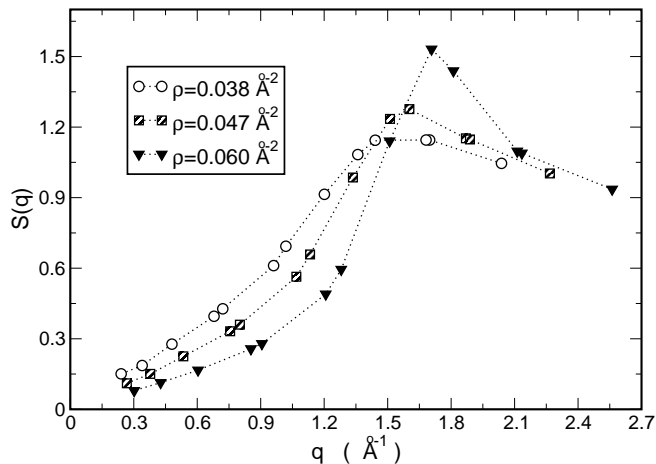


Figure 4: The Static Structure Factor of 2D ${}^3\text{He}$ estimated via the approximate relation $S(q) = F_1(q, \tau = 0)$. (Circles) $\rho = 0.038 \text{ \AA}^{-2}$; (Squares) $\rho = 0.047 \text{ \AA}^{-2}$; (Triangles) $\rho = 0.060 \text{ \AA}^{-2}$. The statistical uncertainties are below the symbol size. The dashed lines are guides to the eye. For a fictitious system of bosons of mass m_3 the results (not shown) deviate from their fermionic counterpart by less than the symbol size.

broadening of the ZSM. The ZSM dispersion $E(q)$ as a function of the wave-vector q can be inferred from the distance between the maximum in $S_2(q, \omega)$ and the value of the energy gap between the Fermionic and the Bosonic ground state, which corresponds to the horizontal line in Fig. 3. The dispersion of the ZSM recalls the classical phonon-maxon-roton mode in bulk superfluid ${}^4\text{He}$; the roton energies decreases with the density and the minimum moves to higher wave-vectors similarly to what happen for the bosonic liquid. Maxon energies increases with the density and also the zero sound velocity has the same trend.

As a byproduct of the calculation of $S(q, \omega)$ we also obtain the static structure factor $S(q)$ and the static density response function $\chi(q)$ from the moments 0 and -1, shown in Figs. 4 and 5, respectively. The QMC evaluation of $S(q)$ is relatively standard and data for liquid ${}^3\text{He}$ have been provided²⁴. On the other hand, we are unaware of previous QMC results for $\chi(q)$. We have also calculated the static response of the fictitious bosonic system, which is significantly less structured than the fermionic counterpart, as expected (see Fig. 5). The static structure factor instead shows very little dependence on the statistics in the density range explored.

Conclusions: In this work we have presented an *ab-initio* estimation of the coherent dynamic structure fac-

tor of 2D liquid ${}^3\text{He}$, a strongly interacting Fermi liquid, combining unbiased QMC sampling techniques with a statistical method¹³ for the analytical continuation from imaginary time to real frequencies under the only approximation (4) ($\psi_0^F \simeq \mathcal{D}\psi_0^B$).

We find a well defined collective mode (the zero-sound mode) at small wavevector; its dispersion relation follows a phonon-maxon-roton pattern, with a significant

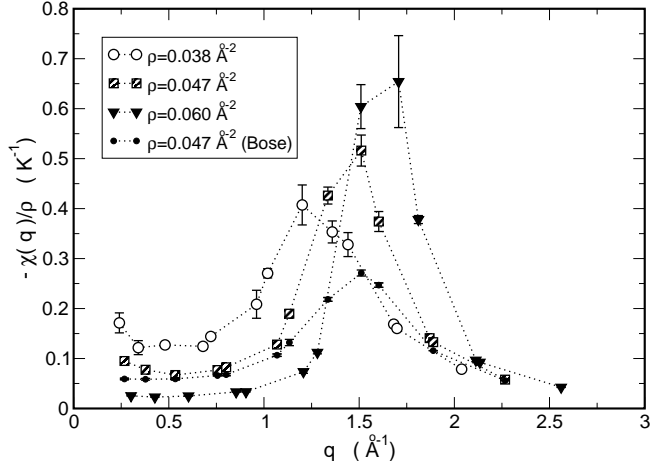


Figure 5: The static response function of ${}^3\text{He}$ obtained from $\chi_q = -2\rho \int d\omega \frac{S(q, \omega)}{\omega}$. (Circles) $\rho = 0.038 \text{ \AA}^{-2}$; (Squares) $\rho = 0.047 \text{ \AA}^{-2}$; (Triangles) $\rho = 0.060 \text{ \AA}^{-2}$. The filled circles show the results for a fictitious system of bosons of mass m_3 at $\rho = 0.047 \text{ \AA}^{-2}$.

broadening in the intermediate wavevector range due the mixing with the particle-hole continuum. These features, including the shape and width of the spectra, are in close agreement with a recent neutron scattering experiment^{3,4}.

We expect that the approximation (4), as suggested by the accuracy of our results for 2D liquid ${}^3\text{He}$ (See Fig. 1), is a good one whenever the effects of quantum statistics are dominated by strong interactions. The formalism can be readily generalized by replacing the density fluctuations operator $\rho_{\vec{q}}$ to access other spectral properties such as spin fluctuations or particle-hole excitations.

Acknowledgements: This work has been supported by CASPUR, Regione Lombardia and CILEA Consortium through a LISA Initiative (Laboratory for Interdisciplinary Advanced Simulation) 2010 grant [http://lisa.cilea.it], and by a grant “Dote ricerca”: FSE, Regione Lombardia.

¹ D. Pines, *Phys. Today* **34**, 106 (1981).

² H.M. Böhm, E. Krotscheck, M. Panholzer, H. Godfrin, H.J. Lauter, M. Meschke, *J. Low. Temp. Phys.* **158**, 194-200 (2010).

³ H.M. Böhm, E. Krotscheck, M. Panholzer, H. Godfrin, H.J. Lauter, M. Meschke, *J. Low. Temp. Phys.* **158**, 147 (2010).

⁴ H. Godfrin, M. Meschke, H.J. Lauter, A. Sultan, H.M.

- Böhm, E. Krotscheck, M. Panholzer *Nature* **483**, 576 (2012).
- ⁵ P.A. Whitlock, G.V. Chester, B. Krishnamachari, *Phys. Rev. B* **58**, 8704 (1998).
- ⁶ M.C. Gordillo, D.M. Ceperley, *Phys. Rev. B* **58**, 6447 (1998).
- ⁷ M. Nava, A. Motta, D.E. Galli, E. Vitali, S. Moroni, *Phys. Rev. B* **85**, 184401 (2012).
- ⁸ R.H. Glyde, in *Excitations in liquid and solid Helium*, Oxford University Press (New York, 1994).
- ⁹ D.M. Ceperley, *Rev. Mod. Phys.* **67**, 279 (1995).
- ¹⁰ S. Baroni and S. Moroni, *Phys. Rev. Lett.* **82**, 4745 (1999).
- ¹¹ R.A. Aziz, V.P.S. Nain, J.S. Carley, W.L. Taylor, G.T. McConville, *J. Chem. Phys.* **70**, 4330 (1979).
- ¹² M. Boninsegni, D.M. Ceperley, *J. Low Temp. Phys.* **104**, 339 (1996).
- ¹³ E. Vitali, M. Rossi, L. Reatto, D.E. Galli, *Phys. Rev. B* **82**, 174510 (2010).
- ¹⁴ M. Rossi, E. Vitali, L. Reatto, D.E. Galli, *Phys. Rev. B* **85**, 014525 (2012).
- ¹⁵ S. Saccani, S. Moroni, E. Vitali, M. Boninsegni, *Mol. Phys.* **109**, 23 (2011); S. Saccani, S. Moroni, M. Boninsegni, *Phys. Rev. Lett.* **108** 175301 (2012).
- ¹⁶ M. Nava, D.E. Galli, M.W. Cole, L. Reatto, *J. Low Temp. Phys.*, DOI 10.1007/s10909-012-0770-9 (2012).
- ¹⁷ M.A. Lee, K.E. Schmidt, M.H. Kalos, and G.V. Chester, *Phys. Rev. Lett.* **46**, 728 (1981); K.E. Schmidt and M.H. Kalos, in *Monte Carlo Methods in Statistical Physics II*, ed. K. Binder (Springer Verlag, Berlin, 1984).
- ¹⁸ P.J. Reynolds, D.M. Ceperley, B.J. Alder, and W.A. Lester, *J. Chem. Phys.* **77**, 5593 (1982).
- ¹⁹ D.M. Ceperley, in *Monte Carlo and Molecular Dynamics of Condensed Matter Systems*, Ed. K. Binder and G. Ciccotti (Bologna, Italy, 1996).
- ²⁰ S. Zhang, J. Carlson and J.E. Gubernatis, *Phys. Rev. Lett.* **74**, 3652 (1995).
- ²¹ A. Sarsa, K.E. Schmidt and W.R. Magro, *J. Chem. Phys.* **113**, 1366 (2000).
- ²² M. Rossi, M. Nava, L. Reatto, and D.E. Galli, *J. Chem. Phys.* **131**, 154108 (2009).
- ²³ D.E. Galli and L. Reatto, *Mol. Phys.* **101**, 1697 (2003).
- ²⁴ J. Boronat, J. Casulleras, V. Grau, E. Krotscheck, and J. Springer *Phys. Rev. Lett.* **91**, 085302 (2003).